

# Protection of center-spin coherence by dynamically polarizing nuclear spin core in diamond

Gang-Qin Liu,<sup>1,\*</sup> Qian-Qing Jiang,<sup>1,\*</sup> Yan-Chun Chang,<sup>1</sup> Dong-Qi Liu,<sup>1</sup> Wu-Xia Li,<sup>1</sup>  
Chang-Zhi Gu,<sup>1</sup> Hoi Chun Po,<sup>2</sup> Wen-Xian Zhang,<sup>3</sup> Nan Zhao,<sup>4</sup> and Xin-Yu Pan<sup>1,†</sup>

<sup>1</sup> *Beijing National Laboratory for Condensed Matter Physics,  
Institute of Physics, Chinese Academy of Sciences, Beijing 100190, China*

<sup>2</sup> *Department of Physics, The Chinese University of Hong Kong, Shatin, New Territories, Hong Kong, China*

<sup>3</sup> *School of Physics and Technology, Wuhan University, Wuhan, Hubei 430072, China*

<sup>4</sup> *Beijing Computational Science Research Center, Beijing 100084, China*

(Dated: May 25, 2022)

We experimentally investigate the protection of electron spin coherence of nitrogen vacancy (NV) center in diamond by dynamical nuclear polarization. The electron spin decoherence of an NV center is caused by the magnetic field fluctuation of the  $^{13}\text{C}$  nuclear spin bath, which contributes large thermal fluctuation to the center electron spin when it is in equilibrium state at room temperature. To address this issue, we continuously transfer the angular momentum from electron spin to nuclear spins, and pump the nuclear spin bath to a polarized state under Hartman-Hahn condition. The bath polarization effect is verified by the observation of prolongation of the electron spin coherence time ( $T_2^*$ ). Optimal conditions for the dynamical nuclear polarization (DNP) process, including the pumping pulse duration and depolarization effect of laser pulses, are studied. Our experimental results provide strong support for quantum information processing and quantum simulation using polarized nuclear spin bath in solid state systems.

PACS numbers: 76.70.Fz, 03.65.Yz, 03.67.Lx, 67.30.hj

Quantum information processing requires qubits that can be initialized, controlled and readout with high fidelity. Furthermore, the quantum coherence of qubits should persist for a long time to realize multiple gate operations on them [1]. However there exists inevitable noise from the environment that causes decoherence of the qubits. Many efforts have been done to protect the qubit from the noise.

Two major strategies have been proposed to enhance the coherent time of qubits, namely, dynamical decoupling (DD) [2]-[5] and dynamical nuclear polarization (DNP)[6]-[8]. DD can average out the fluctuation of the spin bath by flipping center spin state, thus could effectively cut off the interaction between the center spin and its surrounding spin bath. For DNP method, in the ideal case, the nuclear spin bath is prepared in a spin polarized state, and the thermal fluctuation is completely suppressed. In this case, the electron spin could have long coherence time even in the absence of spin echo control (i.e.  $T_2^* \sim T_2$ ).

DD can be used to protect the coherence of NV electron spin [9], [10] but, in general, DD sequences like CPMG or UDD, do not commute with quantum gate operations, so one cannot realize gate operations on the protected spin during DD sequence unless special designed pulses are applied [11], [12]. On the contrary, if one uses DNP to generate a polarized nuclear spin bath, the center spin state can be well protected and manipulated under the polarized surrounding bath, leading to full exploitation of the center spin coherence [6], [13] and [14]. Furthermore, the small magnetic moment of nucleus (3 orders smaller than electron spin) makes the bath polarization persist for a very long time. The polarized nuclear spins are important quantum resources for quantum information processing and quantum simulation applications [15].

Figure 1 shows the general idea of this paper. Firstly, a

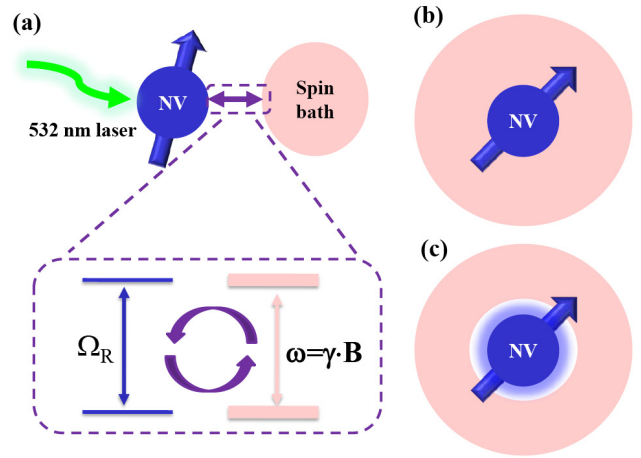


FIG. 1: (Color online) General Schematic. (a) Polarization transformation around an NV center in diamond. Inset, the Hartman-Hahn condition [see Eq.(1)]. (b) Spin bath without DNP, the pink shadow area represents the unpolarized  $^{13}\text{C}$  nuclear spins in thermal equilibrium. (c) After DNP process, the  $^{13}\text{C}$  nuclear spins close to the NV center are polarized (the area in light blue).

short ( $\sim \mu\text{s}$ ) laser pulse is used to polarize the electron spin; which serves as injection of spin polarization. Then, the electron spin is brought to contact with the nuclear spin bath, so that the angular momentum can transfer from the electron spin to the bath. An efficient transfer channel is built up by driving the electron spin with the Hartman-Hahn condition [16](see below), where the nuclear spins are resonant with the electron spin in the rotating frame. The polarization of the bath spins is verified by the enhancement of the electron spin coherence time. If the surrounding bath spins are not polarized

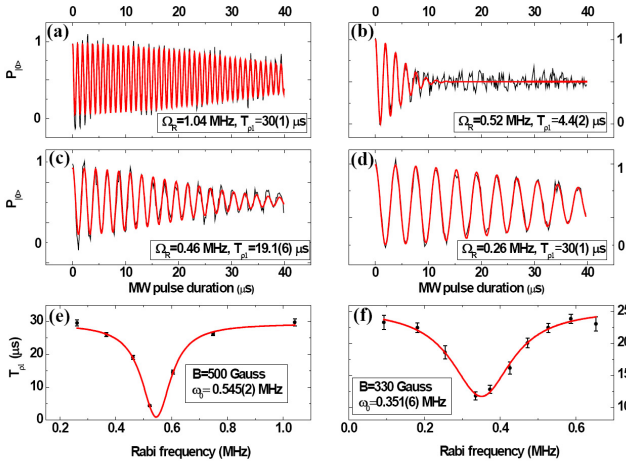


FIG. 2: (Color online) Hartman-Hahn resonance between electron spin and nearby  $^{13}\text{C}$  nuclear spins. (a-d) Rabi oscillation of central electron spin driven by different MW power under  $\mathbf{B}=500$  Gauss. (e) Dependence of the envelope decay time ( $T_{p1}$  time) on the Rabi frequency. A dramatic decay was observed at the Hartman Hahn condition ( $\Omega_R = \gamma_C \mathbf{B} = 545$  kHz). (f) the same as e, with a different magnetic field  $\mathbf{B} = 330$  Gauss ( $\Omega_R = \gamma_C \mathbf{B} = 352$  kHz).

[Fig. 1b], the thermal fluctuation of the bath spins induces a fast decoherence of the central spin. However, when the nuclear spins in the surrounding core are polarized [Fig. 1c], the thermal fluctuation is greatly suppressed. The central spin is effectively isolated from the bath spins, and the quantum coherence can persist for a longer time [8].

The key point for realizing the DNP is to build up an efficient polarization transfer channel [16]. Generally speaking, for two spins with different precession frequencies, the angular momentum transfer process is inefficient due to the energy mismatch. In order to overcome the energy mismatch, one can drive the spins, and adjust the driving power (or Rabi frequency), so that they are in resonance in the rotating frame [17] [18]. In our experiment, we drive the electron spin with microwave pulses, and tune the Rabi frequency ( $\Omega_R$ ) of electron spin to satisfy the Hartman-Hahn condition.

$$\Omega_R = \gamma_C \mathbf{B} \quad (1)$$

Where  $\mathbf{B}$  is the magnetic field and  $\gamma_C = 6.73 \times 10^7 \text{ T}^{-1}\text{s}^{-1}$  is the gyromagnetic ratio of  $^{13}\text{C}$ . In this case, the Rabi frequency is in resonance with the Larmor frequency of the  $^{13}\text{C}$  bath spins under a certain external magnetic field [see the insert figure of Fig. 1a]. Physically, the energy mismatch is compensated by the microwave driving power, and the angular momentum transfer process can occur efficiently.

We experimentally demonstrate this effect by using an NV center in pure single crystal diamond (with Nitrogen concentration  $\ll 5$  ppb). To enhance the photon collection efficiency, a  $12 \mu\text{m}$  diameter solid immersion lens (SIL) is etched above the selected NV [19]. A coplanar waveguide (CPW) antenna

with  $40 \mu\text{m}$  gap is deposited close to the SIL, which can deliver microwave pulses to NV center with high efficiency. A permanent magnet is used to generate the external magnetic field ( $\sim 10^2$  Gauss) along [111] direction of the crystal. The magnetic field lifts the degeneracy of the  $m_S = \pm 1$  states of the electron spin; on the other hand, the host  $^{14}\text{N}$  nuclear spin is also polarized to the  $m_I = +1$  sublevel by the excited state level anti-crossing (ESLAC)[20] under such magnetic field. Thus we have a pure two-level system in the region of weakly driven Rabi oscillation [See SI for details]. To demonstrate the controllable transfer of spin polarization, we change the power of microwave pulse, and measure the decay behavior of Rabi oscillation. Figure 2 shows that the amplitude decay rate of the Rabi oscillation strongly depends on the microwave power. In particular, when the Hartman-Hahn condition is fulfilled, the amplitude decay rate of Rabi oscillation is drastically increased. While in the off-resonant regions, either  $\Omega_R \gg \gamma_C \mathbf{B}$  or  $\Omega_R \ll \gamma_C \mathbf{B}$ , the Rabi oscillation amplitude decays at much slower rate, indicating that the polarized center spin is well isolated from the surrounding bath spins. We fit the Rabi oscillation envelop, and extract the characteristic decay time  $T_{p1}$ . The dependence of decay time  $T_{p1}$  on Rabi frequency  $\Omega_R$  under different magnetic fields is summarized in Fig.2 e& f). The decrease of  $T_{p1}$  under Hartman-Hahn condition is caused by the resonant flip-flop process between nuclear bath spins and the electron spin in the rotating frame. While outside the resonant regime, the direct flip-flop process is suppressed, and only the much weaker second-order processes contribute to decay of the Rabi oscillation amplitude [21].

We now turn to the DNP of surrounding nuclear spin bath. Fig. 3a shows the pulse sequence. A short 532 nm laser pulse (typically  $3 \mu\text{s}$ ) polarizes the center electron spin to  $m_S = 0$  state with high fidelity (95% [11]). A  $\pi/2$  MW pulse rotates the state to the x direction in the equatorial plane of its Bloch sphere. A following 90-phase-shifted MW pulse with the same frequency locks the center spin state along the x direction in the rotating frame for a period of time  $\tau$ . The power of the spin-lock pulse is adjusted to match the HHDR condition, thus the optical pumped high polarization of center spin will transfer during the spin-lock pulse. After that, another laser pulse is used to polarize the center spin again. These polarization injection and transfer processes are repeated  $N$  times, so that a significant nuclear spin polarization is built up in the bath. Finally, we check the polarization effect by measuring the Ramsey interference.

Fig. 3c shows the enhancement of  $T_2^*$  time under DNP. In an external magnetic field of 660 Gauss, with  $N = 10$  times DNP pumping pulses inserted before the Ramsey measurement sequence, the electron spin coherence shows a Gaussian shape decay with a characteristic decay time  $T_2^* = 6.45(7) \mu\text{s}$ . In comparison, the Ramsey signal without DNP decays faster with  $T_2^* = 4.46(6) \mu\text{s}$  (Fig. 3b). The fast oscillation is caused by the strongly coupled nearby  $^{13}\text{C}$  nuclear spin. The enhancement of the  $T_2^*$  time confirms that the DNP sequences suppress the thermal fluctuation of the nuclear spin bath. Fig.

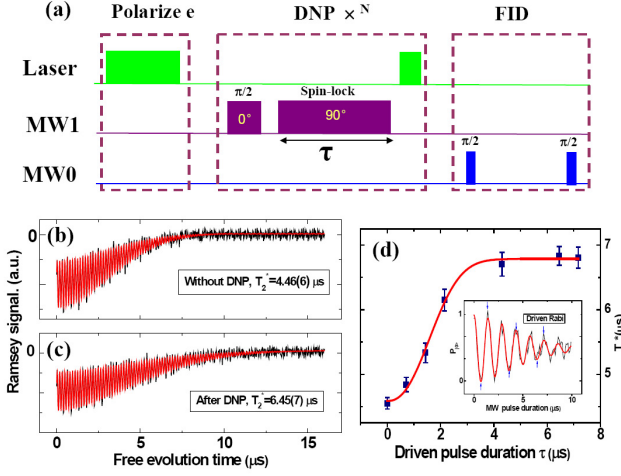


FIG. 3: (Color online) DNP pulse sequence and enhancement of  $T_2^*$  time. (a) The pulse sequence used to generate (the DNP sequence) and to examine (the FID sequence) the nuclear spin bath polarization. (b) FID without DNP. (c) FID after DNP, the prolongation of the dephasing time indicates that the bath spin is polarized during the DNP process. (d) Dependence of the  $T_2^*$  time on the DNP pumping duration, with  $N=10$  (Insert: driven Rabi). The magnetic field is 660 Gauss for these measurements.

3d presents the dependence of electron spin decoherence time on the spin-lock duration  $\tau$ . We find a typical  $2 \mu\text{s}$  lock time is sufficient to transfer the center spin polarization, and longer lock time has little improvement since  $T_2^*$  saturates at  $3 \mu\text{s}$ . The limitation of the dephasing time is determined by the depolarizing dynamics of the bath spins, including the influence of the laser pulse, the fluctuation of the external magnetic field and so on.

We investigate the influence of laser power on DNP effect. The laser pulses with power ranging from  $50 \mu\text{W}$  to  $1.3 \text{ mW}$  were used to carry out the same measurement sequence as shown in Fig. 3a. The optical readout time for electron spin states is also adjusted to ensure high readout fidelity in different laser power. For a fair comparison, free induction decays under the same condition are also measured and plotted [See SI for details.]. As depicted in Fig. 4a, the enhancement of electron spin dephasing time are observed for all the 4 measured cases, and lower laser power gives longer decoherence time, which implies that the possible depolarization effect during the excitation of the NV center electron. Fig. 4b shows the longest coherence time we observed for this NV under the same magnetic field after optimizing the laser power ( $50 \mu\text{W}$  was used). The observed  $T_2^* = 8.0(2) \mu\text{s}$  is nearly two times compares to the dephasing time without DNP.

To further characterize the influence of laser pulse, we insert an extra laser pulse ( $100 \mu\text{s}$ ) between the DNP and the standard FID probe pulse (Fig. 4c). The measured result is presented by Fig. 4d, the resultant dephasing time  $T_2^* = 4.9(2) \mu\text{s}$  is just a little longer than the dephasing time without DNP pulses (Fig. 3b), indicates the nuclear spin bath polarization build by DNP process is significantly destroyed

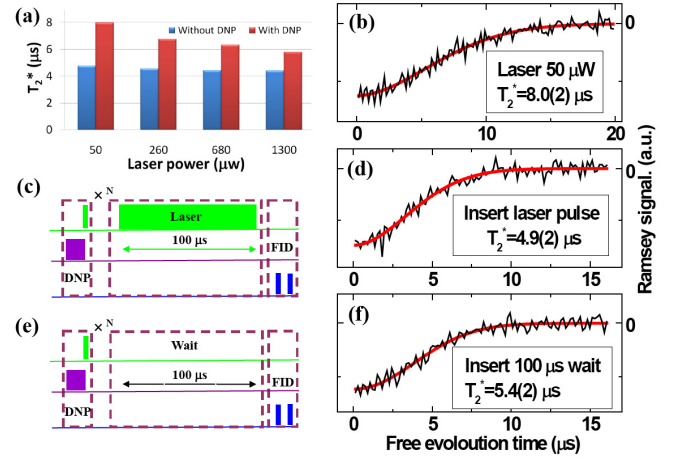


FIG. 4: (Color online) Influence of laser pulse. (a) Laser power Dependence. The (red) blue columns are the  $T_2^*$  times measured with (without) DNP pumping process under 4 different laser power. (b) The FID result with DNP pumping at the optimized laser power ( $50 \mu\text{W}$ ). The  $T_2^*$  time of electron spin is  $\sim 2$  times longer than the case without DNP pumping. (c-d) Pulse sequence and result of adding depolarizing laser pulse. The insertion of laser pulses will depolarize the bath spin polarization built by DNP process, and result in a dephasing time close to the case without DNP. (e-f) Pulse sequence and result of adding waiting time during DNP process. The extra waiting time decreases the effective number of DNP circle, so an in-between dephasing time is observed.

by the laser pulse. A comparison pulse sequence with the laser pulse replaced by a free period (Fig. 4e) gives a long time  $T_2^* = 5.4(2) \mu\text{s}$  (see Fig. 4f) than the case shown in Fig. 4d. Since the nuclear bath spins evolve in a time scale of hundreds of microseconds, and the FID probe sequence takes only several microseconds, the adjacent DNP interact with each other in repetitive measurement, thus the effective number  $N'$  for the continuous measurement is larger than  $N$ . When the  $100 \mu\text{s}$  waiting pulse is inserted between the DNP and FID sequence, the overlapped influence of adjacent DNP sequences become weaker, and the effective number  $N'$  decrease, thus the electron spin dephasing time is shorter than that obtained with continuous measurement.

**Conclusions** We observed the polarization transfer between center electron spin and  $^{13}\text{C}$  nuclear bath spins under Hartman-Hahn condition, and investigated the  $^{13}\text{C}$  nuclear spin dynamical polarization effect. Nearly 2 times longer center spin dephasing time has been observed. The polarization of the spin bath can be built in several microseconds in continuous measurement and persist for hundreds of microseconds. We also found lower power laser pulse could lead to gave longer dephasing time. These findings could potentially open a new way to investigate the dynamics of spin bath.

This work was supported by National Basic Research Program of China (973 Program project Nos. 2009CB929103 and 2009CB930502), the National Natural Science Foundation of China (Grants Nos. 10974251, 91123004, 11104334,

50825206 and 11275139).

*Authors' Note:* During the preparation of this manuscript, we got aware of a similar investigation [22] in which the Hartmann-Hahn condition was used to investigate the  $^{13}\text{C}$  DNP in large magnetic fields. We thank Fedor Jelezko for the helpful discussion.

---

\* These authors contribute equally

† Electronic address: [xypan@iphy.ac.cn](mailto:xypan@iphy.ac.cn)

- [1] M. A. Nielsen and I. L. Chuang. Quantum Computation and Quantum Information (Cambridge Univ. Press, 2000).
- [2] M. Ban, J. Mod. Opt. **45**, 2315-2325 (1998).
- [3] L. Viola and S. Lloyd, Phys. Rev. B. **58**, 2733-2744 (1998).
- [4] K. Khodjasteh and D. A. Lidar, Phys. Rev. Lett. **95**, 180501 (2005).
- [5] W. Yang, Z. Y. Wang and R. B. Liu, Front. Phys. **6**(1), 2-14 (2011).
- [6] D. J. Reilly et al. Science **321**, 817 (2008).
- [7] X. D. Xu et al. Nature **459**, 1105 (2009).
- [8] W. X. Zhang et al. Phys. Rev. B. **82**, 045314 (2010).
- [9] G. de Lange, Z. H. Wang, D. Rist, V. V. Dobrovitski and R. Hanson, Science **330**, 60-63 (2010).
- [10] C. A. Ryan, J. S. Hodges and D. G. Cory, Phys. Rev. Lett. **105**, 200402 (2010).
- [11] T. van der Sar et al. Nature **484**, 82-86 (2012).
- [12] X. K. Xu, et al. Phys. Rev. Lett. **109**, 070502 (2012).
- [13] A. Imamoglu, E. Knill and P. Zoller, Phys. Rev. Lett. **91**, 017402 (2003).
- [14] D. Stepanenko, G. Burkard, G. Giedke and A. Imamoglu, Phys. Rev. Lett. **96**, 136401 (2006).
- [15] J. M. Cai, Alex. R. F. Jelezko and M. B. Plenio. Nature Physics **9**, 168-173 (2013).
- [16] S.R. Hartmann and E.L. Hahn, Physical Review **128**, 5 (1962).
- [17] C. Belthangady et al. arXiv:1211.2749v1.
- [18] A. Laraoui and C. A. Meriles, ACS Nano, **7**(4), 3403-3410 (2013).
- [19] L. Marseglia et al. Appl. Phys. Lett. **98**, 133107 (2011).
- [20] M. Steiner, P. Neumann, J. Beck, F. Jelezko and J. Wrachtrup, Phys. Rev. B. **81**, 035205 (2013).
- [21] V.V. Dobrovitski, A.E. Feiguin, R. Hanson, and D. D. Awschalom, Phys. Rev. Lett. **102**, 237601 (2009).
- [22] P. London et al. arXiv:1304.4709v1.